Journal of Environmental Radioactivity xxx (2014) 1–11

Contents lists available at ScienceDirect

Journal of Environmental Radioactivity

journal homepage: www.elsevier.com/locate/jenvrad

Computational modeling of ^{137}Cs contaminant transfer associated with sediment transport in Abukuma River

T. Iwasaki*, M. Nabi, Y. Shimizu, I. Kimura

Laboratory of Hydraulic Research, Graduate School of Engineering, Hokkaido University, N13, W8, Kita-ku, Sapporo 060-8628, Japan

ARTICLE INFO

Article history:
Received 19 November 2013
Received in revised form
8 May 2014
Accepted 18 May 2014
Available online xxx

Keywords:
Radioactive contaminant
^{137}Cs
Sediment transport
Suspended load
Washload
Numerical modeling

ABSTRACT

A numerical model capable of simulating the transfer of ^{137}Cs in rivers associated with transport of fine sediment is presented. The accident at Fukushima Dai-ichi Nuclear Power Plant (FDNPP) released radionuclides into the atmosphere, and after fallout several radionuclides in them, such as radiocesium (^{134}Cs, ^{137}Cs) and radioiodine (^{131}I) were adsorbed on surface soil particles around FDNPP and transported by surface water. To understand the transport and deposition of the radioactive contaminant along with surface soil particles and its flux to the ocean, we modeled the transport of the ^{137}Cs contaminant by computing the water flow and the associated washload and suspended load transport. We have developed a two-dimensional model to simulate the plane flow structure, sediment transport and associated ^{137}Cs contaminant transport in rivers by combining a shallow water flow model and an advection–diffusion equation for the transport of sediment. The proposed model has been applied to the lower reach of Abukuma River, which is the main river in the highly contaminated area around FDNPP. The numerical results indicate that most ^{137}Cs supplied from the upstream river reach with washload would directly reach to Pacific Ocean. In contrast, washload-oriented ^{137}Cs supplied from the upstream river basin has a limited role in the radioactive contamination in the river. The results also suggest that the proposed framework of computational model can be a potential tool for understanding the sediment-oriented ^{137}Cs behavior in rivers.

1. Introduction

The Great East Japan Earthquake of 11 March 2011 seriously damaged infrastructure, buildings and nature in Japan. The most notable damage from the earthquake and subsequent tsunami was the accident at Fukushima Dai-ichi Nuclear Power Plant (FDNPP). As a result of this accident, radionuclides were released from FDNPP into the atmosphere, and a portion of them deposited on the land in a wide area around FDNPP (Fig. 1a). Several radionuclides in them, such as radiocesium (^{134}Cs and ^{137}Cs) and radioiodine (^{131}I), were strongly adsorbed on surface soil particles (Kato et al., 2012). It indicates that the contaminated soils on land surface by this accident would be a main source of the radioactive contaminant transfer in the natural environment. As in the accident at the Chernobyl nuclear power plant (Zheleznyak et al., 1992), the radionuclides adsorbed on soil particles in the watershed are transported with the soil particles to the ocean through the river channel networks. Therefore, the transport of soil particles on the watershed area caused by rainfall, landslides and water flow on the ground surface is an important factor in determining the sediment-bound radiocesium and radioiodine behaviors in the natural environment. Effective decontaminations of the region around FDNPP and future managements related to the contaminant tracing require the evaluation of the impact of radioactive contaminant transport associated with sediment transport from the river basin to the river and ocean area. Cesium-137 adsorbed on soil particles especially has more long-term impact to the environment since the half-life of ^{137}Cs is about 30 y which is longer than the half-life of ^{134}Cs and ^{131}I. Therefore, the long-term behavior of ^{137}Cs in the environment has to be monitored and predicted. Computational models can be a powerful tool for this purpose; hence this study focuses on the modeling of ^{137}Cs transport in rivers.

It is essential to understand the characteristics of ^{137}Cs adsorption by sediment particles in order to model ^{137}Cs contaminant transport associated with sediment transport. He and Walling (1996) showed that small sediment particles preferentially adsorb ^{137}Cs and ^{210}Pb. Because of large specific surface area and

* Corresponding author. Tel.: +81 11 706 6198.
E-mail addresses: t_iwasaki@eng.hokudai.ac.jp (T. Iwasaki), m.nabi@eng.hokudai.ac.jp (M. Nabi), yasu@eng.hokudai.ac.jp (Y. Shimizu), i-kimu2@eng.hokudai.ac.jp (I. Kimura).

http://dx.doi.org/10.1016/j.jenvrad.2014.05.012
0265-931X/

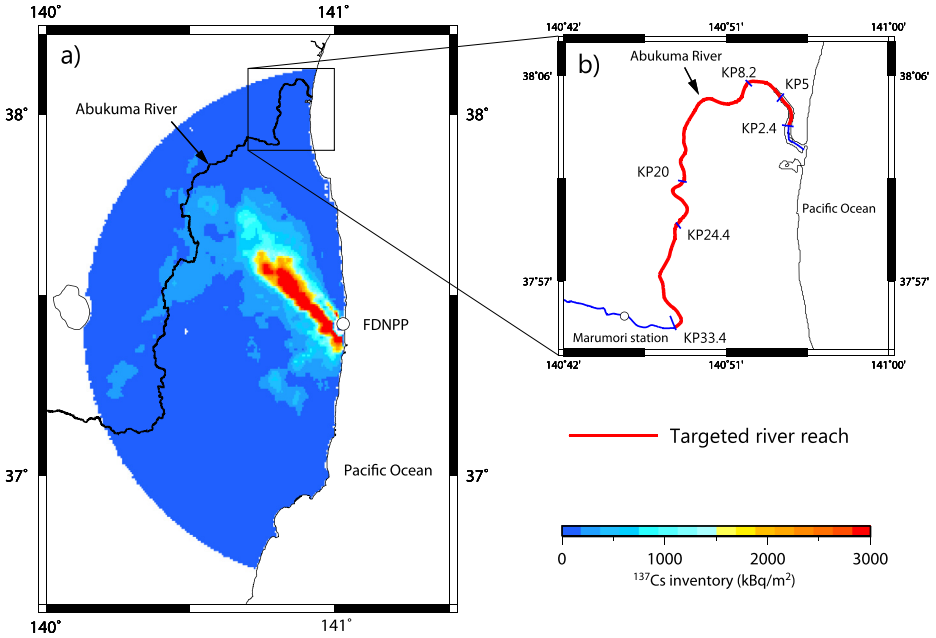

Fig. 1. Location of a) Abukuma River and b) the targeted river reach in present computations. The 3rd Airborne Monitoring Survey Data (http://radioactivity.nsr.go.jp/en/) was used to show the inventory of ^{137}Cs on the land surface in a). KP represents the distance from the river mouth in kilometers.

characteristics of fine sediment, it tends to have higher concentrations of ^{137}Cs than coarse sediments. This suggests that the transport of small sediment particles is a significant part of contaminant transport. Therefore, understanding the movement of fine sediment particles is necessary to determine ^{137}Cs behavior in river environments and the evaluation of contaminant flux to the ocean.

In general, the sediment transport in rivers can be classified into three types: bedload, suspended load and washload. Bedload is the portion of sediment that is transported near the riverbed by rolling, sliding and saltation. Suspended load and washload are sediments that are carried in the water column. Sediment transported as suspended load can actively exchange between the bed and the water column, hence suspended load significantly affects bed evolutions in rivers, especially during flood events. Such large bed evolutions can erode the contaminated soils on the surface of river bed and floodplains. Consequently, the active sediment exchanges between river bed/floodplain and water column have a great role to the transport of ^{137}Cs which are adsorbed on soil particles due to the initial fallout, and also the re-suspension of contaminated sediments in rivers. In contrast, the amount of deposition of sediment transported as washload to the river bed is usually small. In other words, washload has a negligible effect on bed evolutions in rivers. However, since there is a power law relation between flow discharge and sediment concentration in the water column (Glysson, 1987), the flux of washload to the ocean is considerably larger during flood events. Fine sediment particles, which have a small settling velocity, tend to be transported as suspended load or washload, since the shear velocity often becomes large enough during flood events to exceed the sediment settling velocity. This indicates that a large-scale flood can transport to the river, and finally to the ocean, large amounts of suspended load and washload that contain high concentrations of ^{137}Cs contaminants. In addition, although the role of washload to the river bed evolutions is generally small, the washload has an important role in the formation of floodplains (Garcia, 2008). To understand how radioactive contaminants were transported in rivers and were deposited on the river bed and floodplains, it is more important to model the suspended load or washload than to model the bedload. Sediment transport models based on particle techniques are obviously suitable for tracing particle movements in rivers (Cooper et al., 2012). However, it is still not practical to apply Lagrangian models to real rivers for long-term prediction, due to the huge computational efforts. Therefore, Euler-type approaches are preferable. Such approaches generally model the transport of sediment and associated radionuclides by using an advection–diffusion equation with a sink and source term (Onishi, 1981).

This paper proposes a computational model for simulating the ^{137}Cs transport associated with the fine sediments which is usually transported as washload in rivers. A two-dimensional approach has been applied to simulate the behavior of washload-oriented ^{137}Cs in the river and the spatial pattern of deposited ^{137}Cs on the river bed, and estimate the flux of the ^{137}Cs from the river to the ocean. The water flow is simulated by a two-dimensional shallow flow model, and the transport of suspended load is modeled by an advection–diffusion equation with a sink and source term. We applied the proposed model to the lower reach of Abukuma River shown in Fig. 1b, which is the main river in the vicinity of FDNPP accident area (Fig. 1a). Since the ^{137}Cs inventory of the targeted river reach is quite lower than the inventory of the upper reach of Abukuma River, as shown in Fig. 1a, the supplied sediment from the upper reach, which is highly contaminated, might have a crucial impact on the ^{137}Cs behavior in the lower river reach. By using the proposed model, we investigate the role of sediment-oriented ^{137}Cs supplied from the upstream river basin to the lower reach. In addition, the model performance for capturing ^{137}Cs in rivers is discussed by comparing the simulated distribution of deposited ^{137}Cs in the river and the field observation (Japan Atomic Energy Agency, 2013a) taken by an unmanned helicopter (Sanada and Torii, submitted). The transport characteristics of ^{137}Cs associated with washload transport in Abukuma River are discussed based on the budget of ^{137}Cs between the input flux from upstream end, deposition on the bed of the river region, storage in the water column as particulate phase and the outflow flux to Pacific Ocean.

Please cite this article in press as: Iwasaki, T., et al., Computational modeling of ^{137}Cs contaminant transfer associated with sediment transport in Abukuma River, Journal of Environmental Radioactivity (2014), http://dx.doi.org/10.1016/j.jenvrad.2014.05.012

2. Methods

2.1. Computational techniques

Flows in rivers form complex three-dimensional turbulent structures that are difficult to solve with present computational resources. To accurately predict such flows, three-dimensional hydrodynamic models with suitable turbulence closures have to be adopted (Nabi et al., 2012). However, the use of such computational models is limited to research, and those models are employed to understand fundamental micro-scale physical phenomena. It is computationally demanding and inadequate for practical applications associated with river engineering. As a remedy for this obstacle to simulate the real rivers, reduced-dimension models, such as one- or two-dimensional models, have to be applied.

Here, we use a two-dimensional model with a shallow-flow assumption to simulate the flow. The shallow-flow assumption, a hypothesis in which the horizontal scale of the flow is much greater than the vertical scale, allows us to neglect the vertical flow structures (Saint-Venant, 1871). By integrating the three-dimensional hydrodynamic equations, the shallow-flow equations can be derived. The governing equations for the two-dimensional shallow flow in a generalized curvilinear coordinate system are shown as follows (Jang and Shimizu, 2005);

$$\frac{\partial}{\partial t}\left(\frac{h}{J}\right)+\frac{\partial}{\partial \xi}\left(\frac{u^{\xi}h}{J}\right)+\frac{\partial}{\partial \eta}\left(\frac{u^{\eta}h}{J}\right)=0 \tag{1}$$

$$\begin{aligned}&\frac{\partial u^{\xi}}{\partial t}+u^{\xi}\frac{\partial u^{\xi}}{\partial \xi}+u^{\eta}\frac{\partial u^{\xi}}{\partial \eta}+\alpha_1 u^{\xi}u^{\xi}+\alpha_2 u^{\xi}u^{\eta}+\alpha_3 u^{\eta}u^{\eta}\\&\quad=-g\left[\left(\xi_x^2+\xi_y^2\right)\frac{\partial H}{\partial \xi}+\left(\xi_x\eta_x+\xi_y\eta_y\right)\frac{\partial H}{\partial \eta}\right]\\&\qquad-\frac{C_d u^{\xi}}{hJ}\sqrt{\left(\eta_y u^{\xi}-\xi_y u^{\eta}\right)^2+\left(-\eta_x u^{\xi}+\xi_x u^{\eta}\right)^2}+D^{\xi}\end{aligned} \tag{2}$$

$$\begin{aligned}&\frac{\partial u^{\eta}}{\partial t}+u^{\xi}\frac{\partial u^{\eta}}{\partial \xi}+u^{\eta}\frac{\partial u^{\eta}}{\partial \eta}+\alpha_4 u^{\xi}u^{\xi}+\alpha_5 u^{\xi}u^{\eta}+\alpha_6 u^{\eta}u^{\eta}\\&\quad=-g\left[\left(\xi_x\eta_x+\xi_y\eta_y\right)\frac{\partial H}{\partial \xi}+\left(\eta_x^2+\eta_y^2\right)\frac{\partial H}{\partial \eta}\right]\\&\qquad-\frac{C_d u^{\eta}}{hJ}\sqrt{\left(\eta_y u^{\xi}-\xi_y u^{\eta}\right)^2+\left(-\eta_x u^{\xi}+\xi_x u^{\eta}\right)^2}+D^{\eta}\end{aligned} \tag{3}$$

in which;

$$C_d=\frac{gn^2}{h^{1/3}} \tag{4}$$

where, t is the time, ξ and η are the curvilinear coordinates, and u^{ξ} and u^{η} are the contravariant components of depth-averaged velocity in ξ and η-directions, respectively. g is the gravitational acceleration (=9.8 m/s^2), h is the water depth, H is the water level, n is Manning's roughness coefficient, ξ_x, ξ_y, η_x and η_y are the coordinate transformation metrics from the Cartesian coordinate system to a generalized curvilinear coordinate system and J is the Jacobian. Coefficients of α_1 to α_6 are required as result of transforming the velocity components from the Cartesian coordinate system to a generalized curvilinear coordinate system. The velocity components for a moving coordinate system shown by Jang and Shimizu (2005) are neglected because of employing fixed grid system in the present model. D^{ξ} and D^{η} are the turbulent diffusion terms in ξ and η-directions, defined as follows:

$$D^{\xi}=\frac{\partial}{\partial \xi}\left(\nu_t\xi_r^2\frac{\partial u^{\xi}}{\partial \xi}\right)+\frac{\partial}{\partial \eta}\left(\nu_t\eta_r^2\frac{\partial u^{\xi}}{\partial \eta}\right) \tag{5}$$

$$D^{\eta}=\frac{\partial}{\partial \xi}\left(\nu_t\xi_r^2\frac{\partial u^{\eta}}{\partial \xi}\right)+\frac{\partial}{\partial \eta}\left(\nu_t\eta_r^2\frac{\partial u^{\eta}}{\partial \eta}\right) \tag{6}$$

where, ξ_r and η_r are coefficients that show the ratio of local grid size between the generalized curvilinear coordinate system and the Cartesian coordinate system. The eddy viscosity coefficient, ν_t, was evaluated by a zero-equation turbulence closure model as

$$\nu_t=\alpha u_* h \tag{7}$$

where, α is a model constant that is given the value of 0.2 in the present study (Kimura et al., 2009), and u_* is the shear velocity which is calculated by assuming a uniform flow locally with Manning's roughness rule as follows.

$$\left(\frac{u_*}{V}\right)^2=\frac{gn^2}{h^{1/3}} \tag{8}$$

where, V is the absolute depth-averaged velocity.

The evolution of the bed in rivers is the result of erosion and deposition of sediment. Sediment transported near the river bed is called bedload. The main forces controlling bedload transport are gravitation, lift, drag and the force of interparticle collisions. In the case of suspension of sediment, turbulence structures generated in the vicinity of the river bed, such as horseshoe vortices, significantly affect sediment erosion from the river bed and play a great role in the saltation mechanism of sediment particles (Nabi et al., 2013a, b). Turbulence structures such as boils contribute to the suspension of fine material (Venditti and Bennett, 2000; Best, 2005).

The interaction between sediment particles in the water column has only minor importance, because of the relatively low concentration of sediment. Such interaction between the particles is an important factor in the movement of sediment particles near the bed (bedload), because of the high concentration of sediment beside the river bed. The interaction between particles makes the solution of interparticle interaction inherently complex. Considering the suspended load transport as flux is an alternative solution that has been widely used in previous applications (e.g. Kimura et al., 2010). In this technique, the sediment transport in suspension is considered as a flux and solved as concentration. These techniques are computationally efficient and avoid the need for great computational resources. In the present study, we solve only for washload and suspended load, as they are the most important parts in the transport of ^{137}Cs contaminants. The bed evolution and the volumetric conservation of the suspended load can be given by the volumetric balance of the sediment flux.

The bed level can be updated by considering the volumetric balance of suspended load between the upward flux of suspended load from the bed and the settling flux of suspended load by gravity as follows.

$$(1-\lambda)\frac{\partial}{\partial t}\left(\frac{z}{J}\right)=\frac{q_{su}-c_b w_f}{J} \tag{9}$$

where, z is the bed elevation, q_{su} is the volumetric upward flux of suspended load from the bed, c_b is the reference concentration of the suspended load which is defined as the volumetric concentration near the bed, w_f is the settling velocity of the sediment particles and λ is the porosity of the river bed given as 0.4 which is in a range of general value of the river bed (Atkins and Mcbride, 1992), since the governing equations used in this framework

Please cite this article in press as: Iwasaki, T., et al., Computational modeling of ^{137}Cs contaminant transfer associated with sediment transport in Abukuma River, Journal of Environmental Radioactivity (2014), http://dx.doi.org/10.1016/j.jenvrad.2014.05.012

were derived for the case of non-cohesive sedimentary bed. Although three-dimensional flow structures, for instance, sweeps, considerably affects the particle deposition to the river bed (Nino and Garcia, 1996), such effects are completely neglected due to limitation of horizontal two dimensional approaches for computing the flow field used in this study.

The formula proposed by Itakura and Kishi (1980) was applied to evaluate the volumetric upward flux of suspended load from the bed. They derived this formulation based on a dynamics focusing on the turbulence-driven pick-up of sediment particles from the bed and the flume experimental data as follows:

$$q_{su} = K\left(a_* \frac{\rho_s - \rho}{\rho_s} \frac{gd}{u_*} \Omega - w_f\right) \tag{10}$$

with,

$$\Omega = \frac{\tau_*}{B_*} \frac{\int_{a'}^{\infty} \xi \frac{1}{\sqrt{\pi}} e^{-\xi^2} d\xi}{\int_{a'}^{\infty} \frac{1}{\sqrt{\pi}} e^{-\xi^2} d\xi} + \frac{\tau_*}{B_* \eta_0} - 1 \tag{11}$$

$$a\prime = \frac{B_*}{\tau_*} - \frac{1}{\eta_0} \tag{12}$$

where, ρ is the density of water given as 1000 kg/m^3, ρ_s is the density of sediment given as 2650 kg/m^3, τ_* is the Shields number and the model constants have been defined as $\eta_0 = 0.5$, $a_* = 0.14$ and $K = 0.008$.

The settling velocity of the sediment particles was obtained by using the empirical formula proposed by Rubey (1933) as follows.

$$\frac{w_f}{\sqrt{sgd}} = \sqrt{\frac{2}{3} + \frac{36\nu^2}{sgd^3}} - \sqrt{\frac{36\nu^2}{sgd^3}} \tag{13}$$

where, s is the specific weight of sediment in fluid and ν is the kinetic viscosity coefficient given as 0.01 cm^2/s.

The suspended load concentration near the bed herein is obtained with a hypothesis that the vertical profile of the suspended load concentration has an exponential distribution as follows (Wongsa and Shimizu, 2004):

$$c_b = \frac{\beta}{1 - e^{-\beta}} c \tag{14}$$

with,

$$\beta = \frac{6}{\kappa} \frac{w_f}{u_*} \tag{15}$$

where, c is the depth-averaged suspended load concentration and κ is the von Kármán constant (=0.4).

The transport of sediment as washload and suspended load is calculated by using an advection–diffusion equation as follows:

$$\frac{\partial}{\partial t}\left(\frac{ch}{J}\right) + \frac{\partial}{\partial \xi}\left(\frac{u^{\xi} ch}{J}\right) + \frac{\partial}{\partial \eta}\left(\frac{u^{\eta} ch}{J}\right) = \frac{q_{su} - c_b w_f}{J} + \frac{\partial}{\partial \xi}\left(D_t \frac{\partial c}{\partial \xi}\right) + \frac{\partial}{\partial \eta}\left(D_t \frac{\partial c}{\partial \eta}\right) \tag{16}$$

where, D_t is the diffusion coefficient of suspended load concentration in the water column, which is approximated to be equal to ν_t (Rouse, 1937).

In the Basin of Abukuma River, the upper part of watershed area was highly contaminated by the accident of FDNPP as shown in Fig. 1a. Therefore, the soil particles which will be eroded from such land surface have high ^{137}Cs concentration, and will be transported from the river basin to the river channel network. It indicates that the supply of sediment from the upper reach of Abukuma River has an important role in the behavior of ^{137}Cs in the lower river reach. This study focuses on how the sediment is transported from highly contaminated area and affects the ^{137}Cs transport and deposition in the lower reach of Abukuma River. For this purpose, we neglect the initial fallout of ^{137}Cs in the lower reach of Abukuma River and the supply of sediment from different origins such as the tributaries, lateral input and the river bed. In addition, the adsorption/desorption of ^{137}Cs to/from the sediment particle is not taken into account. These assumptions allow us to calculate the deposition amount of ^{137}Cs on the river bed by multiplying the ^{137}Cs concentration in the supplied sediment from the upstream end to the sedimentation rate in the computational cells. The amount of ^{137}Cs deposited in a computational cell can be calculated as follows:

$$D_{cs} = E_{dep}(1 - \lambda) G_{cs} \rho_s \tag{17}$$

where, D_{cs} is the amount of the deposited ^{137}Cs, E_{dep} is the deposited layer thickness of sediment, G_{cs} is the adsorption concentration of the ^{137}Cs on sediment supplied from the upstream boundary.

In solving the governing equations of flow, a finite difference method is applied. A splitting technique is used to solve the shallow-flow equations (Jang and Shimizu, 2005). The continuity equation and the non-advection terms in the momentum equations are solved implicitly, while the advection terms are treated explicitly. A first-order upwinding scheme has been adopted for the advection terms of the momentum equations. To obtain a conservative discretization for the sediment, a finite-volume method has been adopted for solving the advection–diffusion equation of washload and suspended load. A first-order upwinding scheme was also adopted to calculate the flux of washload and suspended load at the cell boundaries to avoid computational instability.

2.2. Study river and model parameterization

The proposed model was applied to Abukuma River, which is the main river in the highly contaminated areas around FDNPP (Fig. 1a). Our target river reach is the lower part of Abukuma River from KP 2.4 to KP 33.4 as shown in Fig. 1b. KP represents the distance from the river mouth in kilometers. The flow close to the downstream end of the river reach is affected by the tidal influence by Pacific Ocean. In the period of 22–24 September 2011, a large-scale flood occurred. The flood was reported to be on a scale comparable to that of the biggest flood on record for Abukuma River (Nippon Koei, 2012). The hydrograph of observed discharge during the flood at Marumori station (Fig. 1b) is shown in Fig. 2 (Water Information System, 2013). Since the large-scale flood had a significant impact on the sediment transport and bed evolution in the river, the amount of ^{137}Cs transport associated with sediment transport might also be large. The hydrograph of observed discharge is given for the upstream boundary. At the downstream boundary, the observed sea level fluctuations were obtained. The average grid dimensions for the computations are 20 m longitudinally by 8.7 m transversely.

Since, for the transport of ^{137}Cs, only the sediment in the water column (washload and suspended load) is taken into account, the concentration of the sediment in water column at the upstream boundary is required in order to obtain the input amount of the sediments. For this purpose, an empirical power law function between the flow discharge and the concentration of sediment was adopted at the upstream end. Fig. 3 shows the relation between the

Please cite this article in press as: Iwasaki, T., et al., Computational modeling of ^{137}Cs contaminant transfer associated with sediment transport in Abukuma River, Journal of Environmental Radioactivity (2014), http://dx.doi.org/10.1016/j.jenvrad.2014.05.012

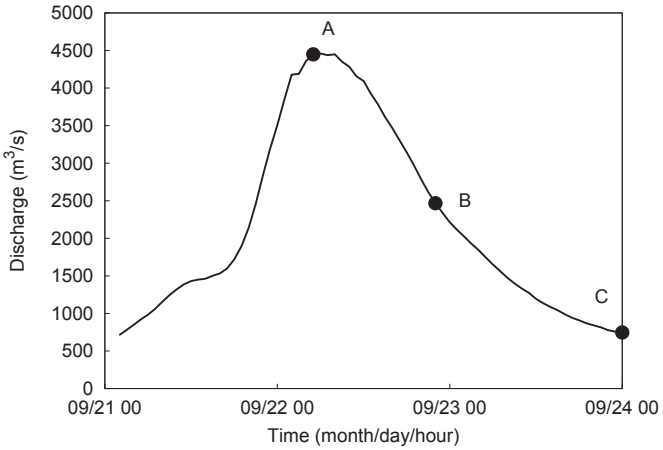

Fig. 2. Hydrograph measured at Marumori station, near the upstream boundary of the selected computation region (see Fig. 1b) on 22 to 24 September, 2011. Times A, B and C correspond to the calculation results shown in this paper.

flow discharge and the concentration of sediments which might include both washload and suspended load at Marumori station measured during the mentioned flood (Nippon Koei, 2012). Although hysteresis feature has been reported between the flow discharge and the concentration of sediments (Smith and Dragovich, 2009), the following relation can be derived from this measurement data at Marumori station.

$$C_{\text{upstream}} = 7.79 \times 10^{-8} Q^{1.02} \tag{18}$$

where C_{upstream} is the volumetric concentration of the sediments at the upstream boundary and Q is the flow discharge. Eq. (18) shows a preferable agreement with the measured data as shown in Fig. 3, and thus the concentration of sediments observed in the flood can be given by using this equation. The sediment in the computation was assumed to have a uniform diameter of 0.0267 mm which is the averaged value of the measured grain size distribution of sediments in the water column during the flood (Nippon Koei, 2012).

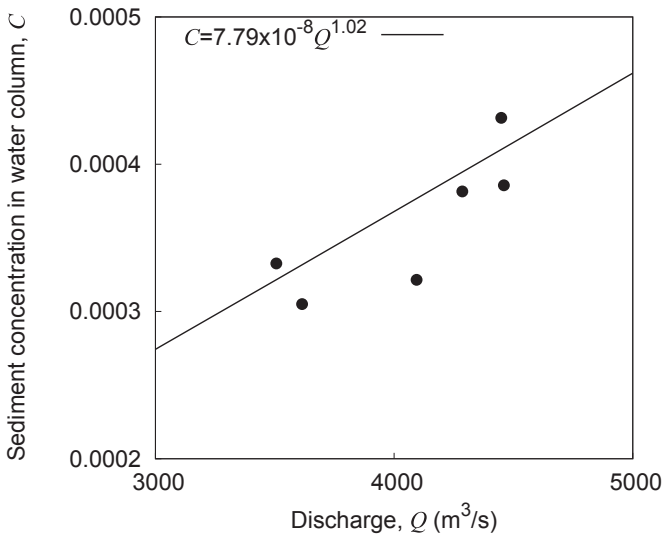

Fig. 3. Relation of flow discharge and the concentration of sediments in the water column measured at Marumori station during the targeted flood (Nippon Koei, 2012). The fitting curve which is a simple power low function shows preferable agreement with the measurement.

As we here deal with ^{137}Cs radionuclides, the concentration of ^{137}Cs in the supplied sediment is the most important parameter in determining the inventory of ^{137}Cs in the river and the flux of ^{137}Cs in the computation. Because of lack in measurement data of ^{137}Cs concentration for that flood, we set the boundary condition for ^{137}Cs concentration using the data of suspended load sampled after the flood, in 7th, December, 2012. The ^{137}Cs concentration of suspended load in this term is in the range from 7 kBq/kg to 11 kBq/kg in this river reach (Japan Atomic Energy Agency, 2013b). On the basis of this measurement data, we herein set the concentration of ^{137}Cs of the supplied sediment from the upstream boundary as 10 kBq/kg.

To provide the initial bed geometry in the computations, the light detection and ranging (LiDAR) data, which are detailed bed elevation data and the cross sectional river bed survey data, were used. In order to give initial bed geometry of the floodplains we used the bed elevation LiDAR data which was measured in May and June, 2011 (CTI Engineering, 2011) with a spatial resolution of 5 m. The cross-sectional survey data of river bed elevation, measured at 200 m longitudinal intervals in 2011 (CTI Engineering, 2012), were used to give the initial bed geometry of river bed where LiDAR data are not available because of existing water. Fig. 4a shows the initial bed elevation in the middle of the river reach, and Fig. 4b is the cross sectional bed geometry at KP24 (see Fig. 1a). The cross sectional bed geometry of Abukuma River is a typical compound channel which consists of a low water channel and floodplains within the river embankment (Fig. 4b). Hereafter, we defined "river bed" as the bed of low water channel, and "floodplains" as the area of both side of the low water channel.

Manning's roughness coefficient in rivers is not constant in space and time. In general, this coefficient has been calculated from the measured water level in order to determine the roughness of the bed surface. For determining Manning's roughness coefficient, we employed one dimensional non-uniform flow equations (e.g. Wu, 2007). By obtaining observed flow discharge, water level and measured bed geometry to the non-uniform flow model, we can calibrate Manning's roughness coefficient which reproduce the observed water level. In this computation, the water level measured in the 1986 flood was used for calibrating Manning's roughness coefficient in the lower reach of Abukuma River. The given Manning's roughness coefficient is shown in Table 1 (CTI Engineering, 2007).

3. Results and discussions

3.1. Transport and deposition of ^{137}Cs

Fig. 5 shows simulated temporal change of several ^{137}Cs fluxes; the supplied flux from the upstream end, outflow flux to the coastal area, storage flux as the particulate matter in the river water and the deposition flux on the bed of the river (low water channel and floodplains). The temporal change of supplied ^{137}Cs flux from the upstream end corresponds to the given flow discharge, since we employed a power law relation to estimate the concentration of the sediments in the water column and constant ^{137}Cs concentration in time. The simulated outflow flux of ^{137}Cs to the coastal area shows mostly a similar temporal variation to that of the upstream end, but includes a time lag. This time lag, between the each peak of the flux, is approximately 4.5 h. It indicates that a major part of the upstream ^{137}Cs, associated with the washload, reaches to the river mouth within 4.5 h. A balance between the supplied and outflow fluxes gives the amount of sediment and related ^{137}Cs which is stored and deposited on the bed of the river.

The budget of ^{137}Cs in the river reach at the end of the computation is shown in Table 2. The percentage of the outflow

Please cite this article in press as: Iwasaki, T., et al., Computational modeling of ^{137}Cs contaminant transfer associated with sediment transport in Abukuma River, Journal of Environmental Radioactivity (2014), http://dx.doi.org/10.1016/j.jenvrad.2014.05.012

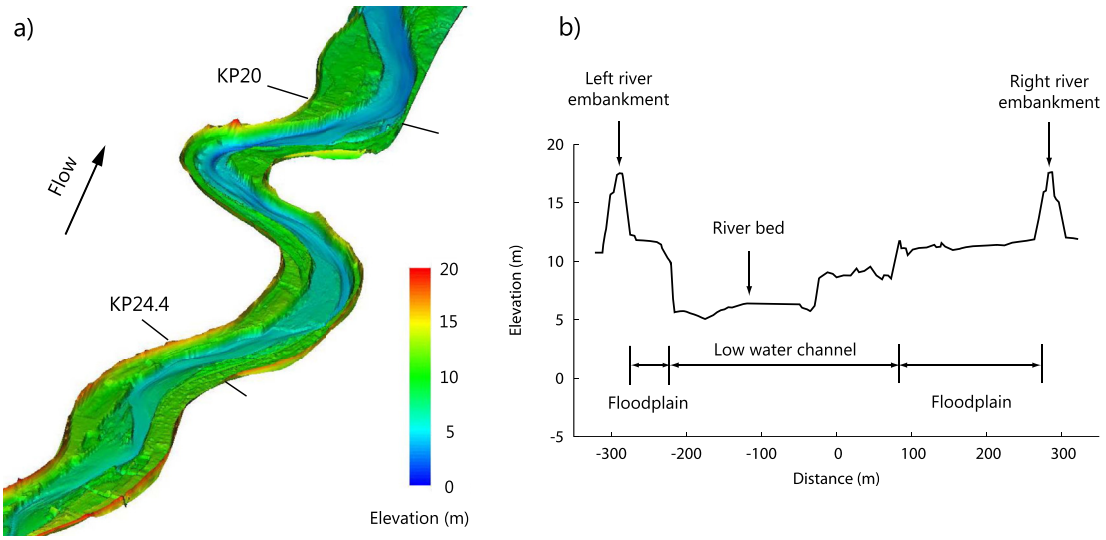

Fig. 4. a) birds eye view of the initial bed geometry in the middle of the targeted river reach (see Fig. 1b), and b) cross-sectional bed geometry in KP24.4. The bed geometry in cross section in Abukuma River shows a typical compound channel, and term of "river bed" and "floodplain" are defined as the bed of low water channel and the floodplain as shown in b).

^{137}Cs flux to the supplied ^{137}Cs flux is about 98.1%, while only 0.77% ^{137}Cs supplied from the upstream end can remains on the bed in the river. Since the deposited amount of ^{137}Cs on the bed is quite small, ^{137}Cs storage associated with the particulate matter in the water is strongly controlled by the balance of the supplied and outflow ^{137}Cs flux. In contrast, it is worth to focus on the temporal change of the deposited amount of ^{137}Cs on the bed of the river reach. In the increasing stage of discharge, the deposition flux of ^{137}Cs becomes negative; it means that the re-suspension of ^{137}Cs is dominated. However, such tendency is limited and ^{137}Cs mostly deposits as shown in Fig. 5. Fig. 5 also indicates that the deposition ^{137}Cs flux to the bed of the river tends to increase during the decreasing stage of discharge.

For the detailed understanding of the ^{137}Cs deposition to the bed of the river, we show the simulated spatial pattern of deposited ^{137}Cs in the river reach in Fig. 6. The results in Fig. 6 are associated with a) near peak discharge, b) the falling stage of discharge hydrograph and c) the end discharge hydrograph, shown by points A, B and C in Fig. 2, respectively. The computational results for peak discharge (Fig. 6a) show that the deposition of ^{137}Cs on the river bed is quite small before the discharge reaches its maximum. A small amount of ^{137}Cs deposition can be found on the floodplain or near the river embankment. However, in the decreasing discharge stage, the inventory of ^{137}Cs on the floodplain increases, as shown in Fig. 6b. The decreasing flow discharge corresponds to the decreasing water level in the river. When the water level on the floodplain decreases, the water depth becomes smaller and the flow velocity decreases; hence, the fine sediment in washload partly deposits on the floodplain. This phenomenon is associated with the relatively low shear velocity that occurs mainly in shallow flows. This low shear stress is insufficient to keep the sediment in suspension. In general, Rouse number, R, is a governing parameter to classify the mode of sediment transport defined as follows:

$$R = \frac{w_f}{\kappa u_*} \tag{19}$$

From the definition of Rouse number, the low shear velocity gives high Rouse number. By using this parameter, we discuss the deposition of the sediments on the river bed and the floodplain, which are supplied as washload from the upstream boundary.

There is a threshold Rouse number determining the mode of sediment transport between washload and suspended load, for instance 0.8 (Hean, 2008). This empirical law has shown that in the flow condition which Rouse number is lower than the threshold value, sediment particles tend to be transported as washload and rarely deposit on the bed. In contrast, the mode of sediment transport may be suspended load in case of high Rouse number, and in this case the sediment particles of suspended load can exchange the sediment with the bed. Since Rouse number is included in both, the volumetric upward flux of suspended load from bed (Eq. (10))

Table 1
Manning's coefficient, n, used in the computations. The locations of KP are shown in Fig. 1b.

Manning's coefficient	KP				
	2.4–5	5–8.2	8.2–20	20–24.4	24.4–33.4
Low-water channel	0.022	0.022	0.025	0.034	0.031
Floodplain	0.055	0.041	0.038	0.036	0.033

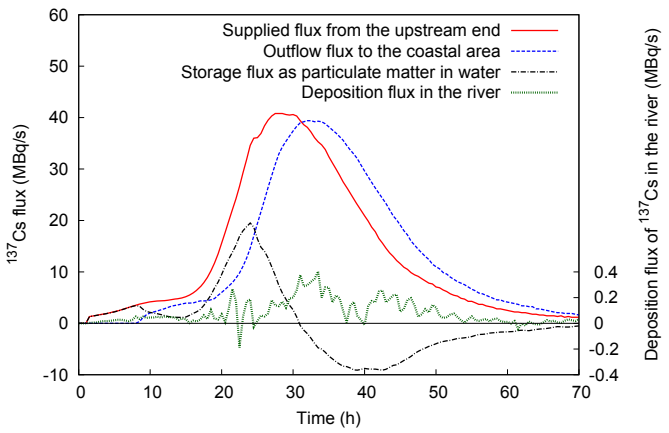

Fig. 5. Temporal changes of several ^{137}Cs flux in the targeted river reach. Left axis is for the supplied flux from the upstream end, the outflow flux to the coastal area and storage flux as particulate matter in water, while right axis is for the deposition flux in the river.

Please cite this article in press as: Iwasaki, T., et al., Computational modeling of ^{137}Cs contaminant transfer associated with sediment transport in Abukuma River, Journal of Environmental Radioactivity (2014), http://dx.doi.org/10.1016/j.jenvrad.2014.05.012

Table 2
The budget of ^{137}Cs in the targeted river reach at the end of computation.

	Amount of ^{137}Cs (GBq)	Percentage to the supplied ^{137}Cs (%)
Supplied from the upstream end	3351	100
Outflow to the coastal area	3288	98.1
Deposition in the river	25.7	0.77
Particulate matter in the water	42.2	1.26

and the vertical profile of suspended load concentration (Eq. (14)), such phenomenon can be captured in the proposed model. Fig. 7 shows the Rouse number dependency to the volumetric upward flux of suspended load from bed and the suspended load concentration near the bed normalized by the depth-averaged concentration under the present condition. Decreasing Rouse number significantly increases the upward flux of suspended load from the bed, and approximates the normalized suspended load concentration near the bed to unit which means the vertical profile of suspended load is uniform. Since the upper limit of Rouse number which corresponds to the critical Shields number given by Iwagaki formula (Iwagaki, 1956) in the present condition is approximately 0.2, and it is significantly smaller than the threshold Rouse number, the mode of sediment transport in the present calculation will be washload or suspended load, after the sediment particle once starts to move.

Fig. 8 shows the computed temporal changes of Rouse number on the floodplain and in the low water channel (defined in Fig. 6a). In the low water channel, the Rouse number is sufficiently small and the sediment transport remains as washload. Therefore, the associated ^{137}Cs cannot deposit on the river bed, as shown in Fig. 6. However, on the floodplain, the Rouse number increases in the falling stage of discharge, and finally the Rouse number becomes over the upper limit. It causes significant deposition of the sediment which is supplied from the upstream boundary as washload, thus, ^{137}Cs deposits on the floodplain. Consequently, the floodplain is partially contaminated by the deposition of fine sediment with a high concentration of ^{137}Cs (Fig. 6c), although the simulated inventory of ^{137}Cs on the floodplain is not considerably high compared with the measured inventory on the ground surface around FDNPP shown in Fig. 1a.

3.2. The spatial pattern of ^{137}Cs deposition on the floodplain

The simulated budget of ^{137}Cs in the river reach shows that the amount of ^{137}Cs deposition on the bed of the river is quite small in comparison to the total supplied ^{137}Cs from the upstream boundary during the flood event. However, this is not equivalent to indicate that the impact of this flood to the ^{137}Cs deposition is negligible. As indicated by the computed results in Fig. 6, parts of floodplain might be contaminated by ^{137}Cs associated with washload deposition. This impact can be roughly found from the airborne monitoring survey of the air dose level around FDNPP before and after the flood, conducted from May to July, 2011 (3rd monitoring) and from October to November, 2011 (4th monitoring), respectively (Ministry of education, culture, sports, science and technology, 2011). Fig. 9a shows the ^{137}Cs inventory estimated by the 3rd monitoring around the river reach, and this inventory corresponds to the measurements before the flood. As shown in Fig. 9a, ^{137}Cs inventory in the river was not considerably high before the flood. The general tendency is that ^{137}Cs inventory in the south part was higher than ^{137}Cs inventory in the north part. The ^{137}Cs inventory before the flood was mainly determined by the initial fallout due to the accident of FDNPP. In contrast, Fig. 9b shows the difference of the ^{137}Cs inventory between 3rd and 4th monitoring survey, which was plausibly caused by the ^{137}Cs deposition during the flood. This figure clearly shows that ^{137}Cs inventory in the river significantly increased after the flood. In addition to these airborne surveys of air dose level, more detailed spatial pattern of ^{137}Cs inventory was estimated from the air dose level measurements by an unmanned helicopter in January, 2013 as shown in Fig. 10a (Sanada and Torii, submitted). Since between FDNPP accident to January 2013 this flood was the solitary flood in which the water level could cover to the floodplains, the difference between the measurements by the helicopter and by the 3rd monitoring survey also corresponds to

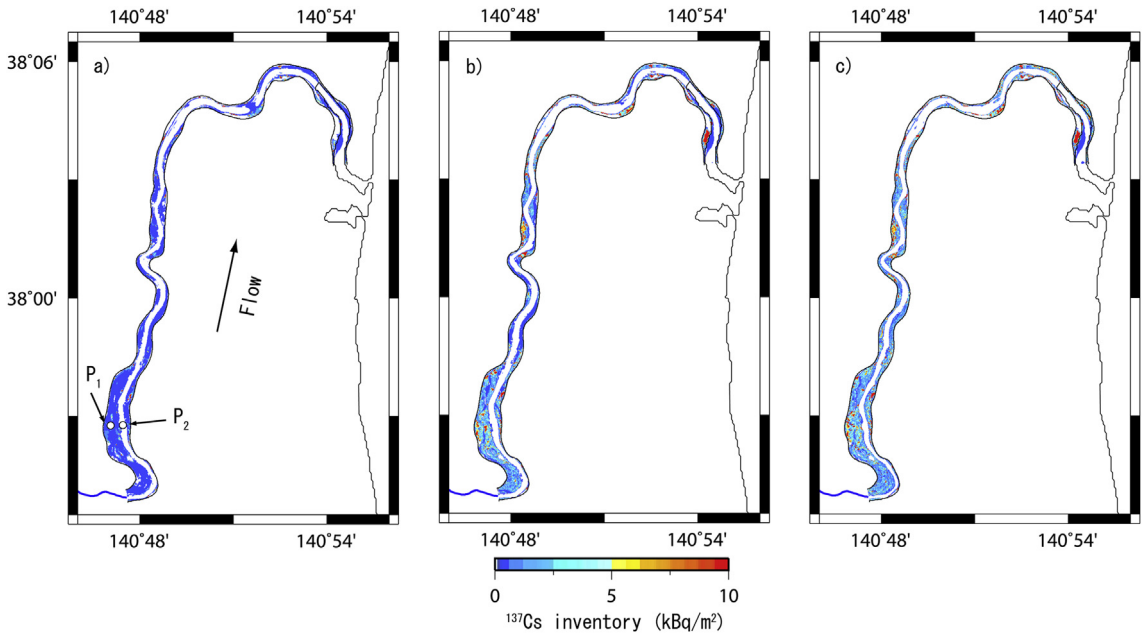

Fig. 6. Simulated spatial distribution of deposited ^{137}Cs in the computation for Abukuma River. Figures a), b) and c) correspond to the calculation results for times A, B and C shown in Fig. 2. P_1 and P_2 are the representative points in the low water channel and floodplain, to show the local features of the calculation results in Fig. 8. The flow direction is from the bottom to top of the figures.

Please cite this article in press as: Iwasaki, T., et al., Computational modeling of ^{137}Cs contaminant transfer associated with sediment transport in Abukuma River, Journal of Environmental Radioactivity (2014), http://dx.doi.org/10.1016/j.jenvrad.2014.05.012

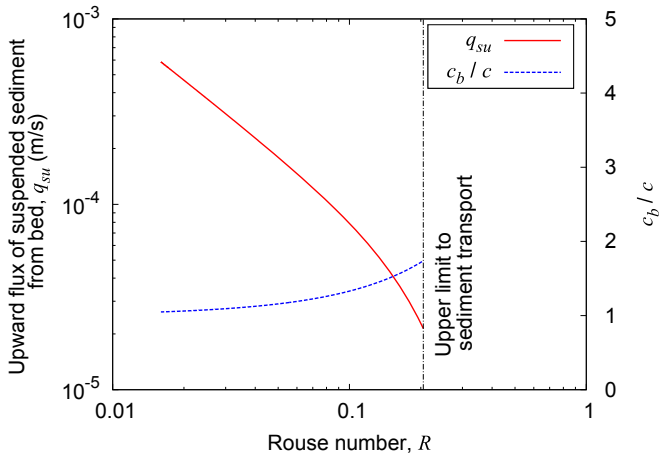

Fig. 7. Rouse number dependency of the volumetric upward flux of suspended load from the bed (red-solid line) and the suspended load concentration near the bed normalized by the depth-averaged suspended load concentration (blue-dash line) in the present condition ($d = 0.0267$ mm, $\rho_s = 2650$ kg/m^3, $\rho = 1000$ kg/m^3, $s = 1.65$). The upper limit of Rouse number to sediment transport which corresponds to the critical Shields number given from Iwagaki formula (Iwagaki, 1956) is about 0.2.

the ^{137}Cs deposition during the flood. This difference, as shown in Fig. 10b, greatly contributes in understanding the detailed spatial pattern of ^{137}Cs deposition during the flood compared to Fig. 9b, and clearly demonstrates that the floodplain in the lower reach of Abukuma River is partially contaminated by ^{137}Cs from the upper reach. These comparisons indicate that the flood might have an important role in ^{137}Cs inventory in the lower reach of Abukuma River. By comparing ^{137}Cs inventory from the simulation and from the measurements, we discuss the model performance in replicating the ^{137}Cs deposition and show the importance of the washload to ^{137}Cs deposition in the river.

Firstly, we compare the total ^{137}Cs inventory after the flood. Since the initial fallout of ^{137}Cs is not included in the simulation, estimated inventory by the helicopter survey, and the sum of simulated inventory and estimated inventory by the 3rd monitoring are compared at the grid point as shown in Fig. 11a. A comparison between measured ^{137}Cs inventory by the helicopter and by the 3rd monitoring is also shown in Fig. 11a. The grid resolution for this comparison is 100 m which is determined from the spatial resolution of the helicopter survey. This figure clearly demonstrates that there is a correlation between the inventory by

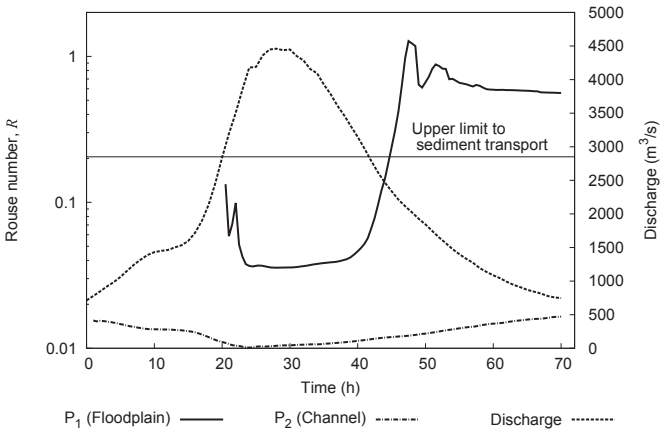

Fig. 8. Temporal changes in Rouse number in the low water channel (P_1) and on the floodplain (P_2). The locations of P_1 and P_2 are shown in Fig. 6a.

the helicopter survey and the 3rd monitoring survey, and the deposition of washload play a minor role in the deposition of ^{137}Cs within the river. This result indicates that the initial fallout, which is not considered in the computation, is a main source of the ^{137}Cs deposition in the river. In addition to this comparison, in order to focus on the role of washload to ^{137}Cs deposition within the river, we compare the computational results with the measured ^{137}Cs deposition during the flood in Fig. 11b. This figure demonstrates quite low correlation between the simulated and measured ^{137}Cs inventory, however, it seems that the relation between the simulated and measured ^{137}Cs inventory shows two trends; partially predicted and totally unpredicted. The simulated results are mostly underpredicted; over 85% points are located under the line of 20% of the measured ^{137}Cs inventory, and these points show quite low correlations. In contrast, some points are located around 50% of the measured ^{137}Cs inventory. It means that in the limited area, the washload deposition has an important role in ^{137}Cs deposition in the river. Fig. 12 shows the spatial distribution of the ^{137}Cs inventory ratio between the simulation and the measurements shown in Fig. 11b. The areas where the ratio of the simulated ^{137}Cs inventory to the measured inventory becomes relatively high are mainly located on the floodplains and in the inner area of bends as shown in Fig. 12 by the arrows. As explained in the previous section, the Rouse number increases sufficiently on the floodplain and deposits the washload in the falling stage of discharge hydrograph. In addition, the inner part of bends on the floodplains would be a dead zone where the Rouse number tends to be large due to flow recirculations (Ferguson et al., 2003). Consequently, such places where Rouse number tend to be sufficiently large for deposition of fine sediments even in flood events may be partially affected by washload-oriented ^{137}Cs supplied from the upstream river reach. These results provide the possibility to specify the accumulation areas of sediment-oriented radioactive contaminants, and thus important information for the continuous decontaminant works in the river.

The low correlation between the washload-oriented ^{137}Cs deposition in the simulation and the measurements is caused by the fact that the initial fallout is a main source for the ^{137}Cs deposition in the river. The resolution of ^{137}Cs inventory measurements by the helicopter survey and the 3rd monitoring is quite different. The spatial resolution is approximately in the order of 100 m for the helicopter survey and few hundred meters for the 3rd monitoring survey. It means that the difference of ^{137}Cs inventory between them is not the exact amount of deposition during the flood. Especially, the low spatial resolution for the 3rd monitoring play a considerable role in diffusing the spatial pattern of ^{137}Cs inventory compared to the inventory by the helicopter survey. Thus, it is hard to extract a detailed pattern of ^{137}Cs deposition during the flood, and the measured ^{137}Cs deposition during the flood (Fig. 10b) would have a considerable error for the present comparison. In order to understand the role of sediment transport in the ^{137}Cs behavior in the river accurately, the detailed measurement to capture the spatial pattern of ^{137}Cs deposition within the river is required.

3.3. Model limitation

The numerical results suggest that the proposed simple model for calculating flow, sediment transport and radiocesium transport can be a potential tool for understanding the sediment-bound radioactive contaminant behavior in the rivers. However, for a detailed understanding of the behavior of radionuclides in the rivers, further improvement of the model is needed. Although in the simulated reach of Abukuma River, the difference of spatial accuracy for measuring the ^{137}Cs inventory by the helicopter and

Please cite this article in press as: Iwasaki, T., et al., Computational modeling of ^{137}Cs contaminant transfer associated with sediment transport in Abukuma River, Journal of Environmental Radioactivity (2014), http://dx.doi.org/10.1016/j.jenvrad.2014.05.012

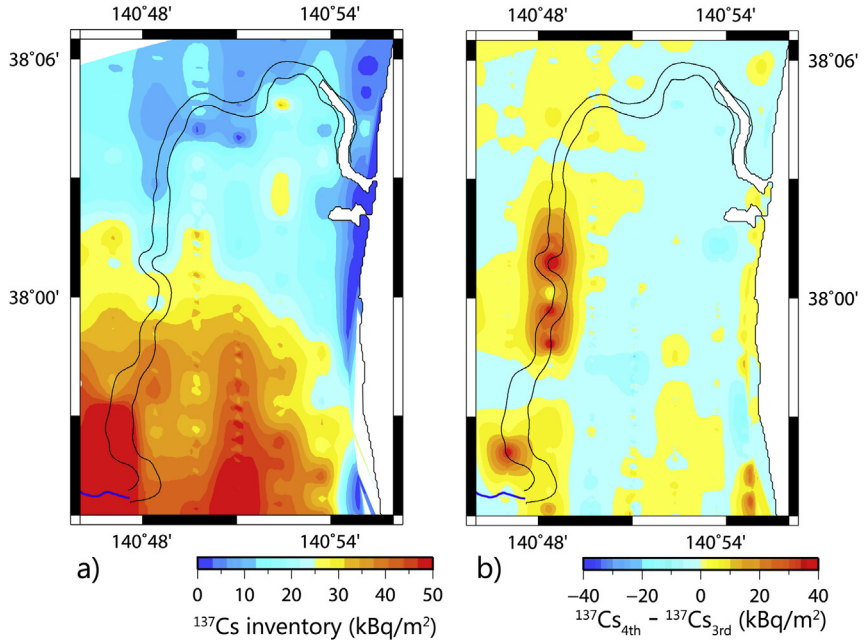

Fig. 9. a) Cesium-137 inventory by 3rd airborne survey of air dose level (http://radioactivity.nsr.go.jp/en/), b) difference of the inventory between 3rd and 4th monitoring survey (Ministry of education, culture, sports and science technology, 2011). $^{137}Cs_{3rd}$ and $^{137}Cs_{4th}$ denote the ^{137}Cs inventory estimated by the 3rd and 4th monitoring survey, respectively.

the 3rd monitoring is a reason for the underestimation, the model used in this computation also has limitations in terms of application to realistic sediment transport phenomena in rivers. In this simulation, the transport of sediment in the water column is modeled as transport of uniform fine sediment. However, because of the grain size dependency for the radiocesium adsorption, considering the grain size distribution of sediment would be important even though the fine sediment particle has high radiocesium concentration. In addition, bedload transport has considerable role in the morphological changes of river bed, for instance, formation and development of ripple, dune, sandbar and meandering. Therefore, the modeling of grain size distribution of sediment is required in realistically capturing sediment transport and bed evolution in rivers, thus understanding the interaction between such morphodynamic phenomena in rivers and the radiocesium behaviors. In addition, the field measurements, focused on radionuclides adsorbed on the sediment particles, suggesting that sediment with small diameter, which is transported as suspended load, also has high concentrations of radionuclides (Tanaka et al., submitted). Although the concentration of ^{137}Cs

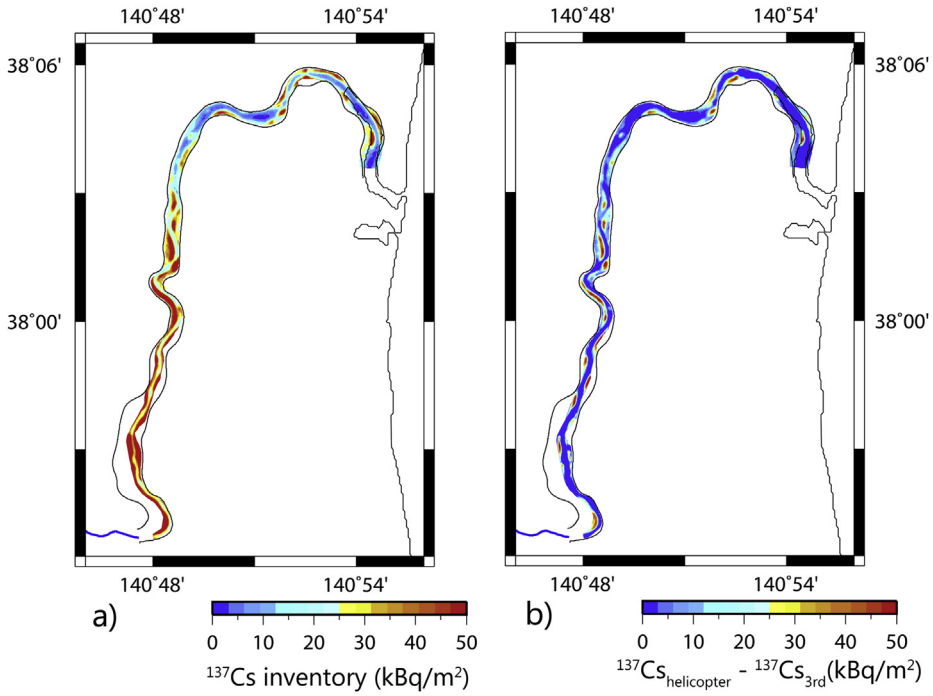

Fig. 10. a) Cesium-137 inventory estimated by an unmanned helicopter survey for the air dose level (Sanada and Torii, submitted) around the targeted river reach, ($^{137}Cs_{helicopter}$) b) difference of the inventory between estimated by the helicopter survey and the 3rd monitoring.

Please cite this article in press as: Iwasaki, T., et al., Computational modeling of ^{137}Cs contaminant transfer associated with sediment transport in Abukuma River, Journal of Environmental Radioactivity (2014), http://dx.doi.org/10.1016/j.jenvrad.2014.05.012

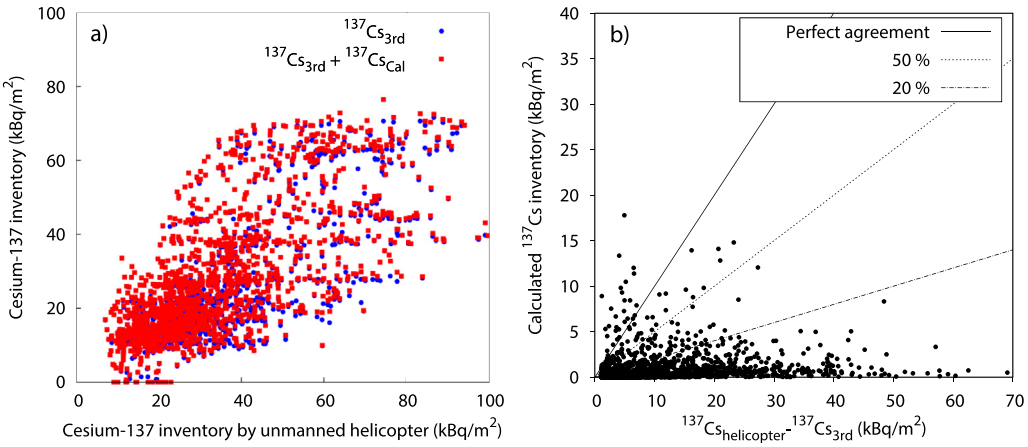

Fig. 11. Comparison of ^{137}Cs inventory, a) between estimated inventory by the helicopter survey, and the sum of calculated inventory ($^{137}Cs_{Cal}$) and estimated inventory by 3rd monitoring, b) between the calculated inventory and the measured inventory during the flood.

associated with sediment in suspended load is less than that in washload, the impact of the transport of radionuclides associated with suspended load on the river and ocean cannot be neglected. Consequently, at least some combination of washload and suspended load transport should be included in the model. This can be realized by the incorporation of a mixed grain size transport model.

A computational issue also exists for long-term prediction of the transport of radioactive contaminants on different spatial scales. The present study simulated only one flood event, with duration of 4 d. Although the two-dimensional approach adopted in this study is a powerful tool for simulating radiocesium transport and deposition in rivers, the computational costs are still large and the computations cannot be applied to large spatial and temporal scales. However, as observed in the accident of Chernobyl nuclear power plant, the runoff rate of radiocesium into the river per a year to the total amount of radiocesium deposited on the surface soils of river basin is merely order of 0.01–1% (International Atomic Energy Agency, 2006). It means that in the river around FDNPP, the transfer of radioactive contaminants associated with sediment transport from river basin to ocean will also continue for a few decades. For a comprehensive understanding of such large-scale, long-term radionuclide transport, different computational techniques are required. One solution is to reduce the computational effort by using one-dimensional approaches. One-dimensional models have been effectively used to simulate longitudinal flow and bed evolution in rivers. Using one dimensional models may greatly contribute to evaluate long-term radiocesium flux to the ocean and amount of radiocesium in the whole river region of river network. However, since one dimensional models deal with cross-sectional averaged flow, sediment transport and bed evolution in rivers, it is hard to discuss the plane distribution of the radiocesium and most importantly the possibility of accumulation of radioactive contaminant in the river reaches. An outcome of this difficulty is to use an effective computational technique by combining one- and two-dimensional models. The one-dimensional model can be used for large-scale simulations, while the two-dimensional model solves the regions where detailed spatial calculations are necessary (Chen et al., 2012). This problem can also be solved by applying parallel computing techniques, using Message Passing Interface. Such models will greatly contribute to simulate the long-term, large-scale problems and temporal and local-scale problems of the radiocesium behavior in rivers spontaneously.

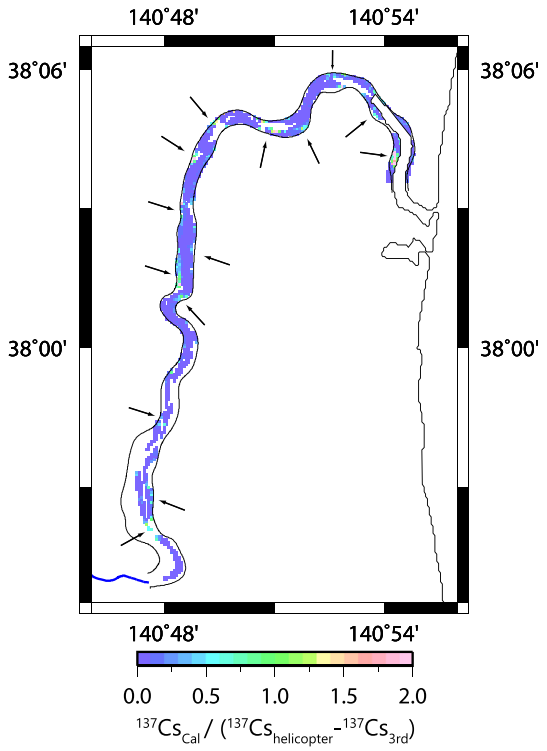

Fig. 12. The ratio of calculated ^{137}Cs inventory to the measured ^{137}Cs inventory during the flood. The arrows show the areas where the agreement between the calculation results and the measurements is relatively high, while in other areas, the model totally unpredicted the measured ^{137}Cs inventory.

Lastly, for an accurate estimation of radioactive contaminant transport and verification of the current model, detailed field measurements are necessary. For instance, the concentration of radionuclides absorbed by the sediment in this simulation is obtained from measurements under usual flow conditions. Because flood events have large impacts on radioactive contaminant transport in the natural environment, data should be measured during the flood events. Detailed field measurements for giving accurate initial and boundary conditions would greatly contribute to the improvement of the model results.

4. Conclusions

This paper presents a computational model for simulating the transport of ^{137}Cs associated with the fine sediment which is generally transported as washload in rivers during flood events on the basis of a plane two-dimensional approach. We applied this model to a large-scale flood event on Abukuma River, which is the

Please cite this article in press as: Iwasaki, T., et al., Computational modeling of ^{137}Cs contaminant transfer associated with sediment transport in Abukuma River, Journal of Environmental Radioactivity (2014), http://dx.doi.org/10.1016/j.jenvrad.2014.05.012

main river in the highly contaminated area around FDNPP, to understand the transport and deposition process of ^{137}Cs and to estimate the flux of ^{137}Cs to Pacific Ocean. The computational results suggest that the supplied ^{137}Cs associated with washload from the upstream river basin would mostly reach to the ocean directly, and deposition amount of ^{137}Cs in the river is quite small. However, the bed surface of floodplain and inner area of river bends are partially contaminated by washload-oriented ^{137}Cs in the decreasing stage of hydrograph, because Rouse number at these area increases sufficient large for depositing the washload to the bed. These results indicate that the washload-oriented ^{137}Cs supplied from the upstream river basin has a limited role to the ^{137}Cs behavior in the river.

For further improvement of the results, the sediment transport and bed evolution model should be extended to a mixed-sediment model for capturing realistically sediment transport phenomena in rivers and understanding the interaction of morphodynamics of river bed and the behavior of radioactive contaminants. In addition, detailed field measurements, for instance the concentration of radionuclides in the sediment during large-scale flood events, greatly contribute to accurate initial and boundary conditions, therefore improving the model results.

References

Atkins, J.E., Mcbride, E.F., 1992. Porosity and packing of Holocene river, dune, and beach sands. AAPG Bull.-Am. Assoc. Petrol. Geol. 76 (3), 339–355.

Best, J., 2005. The fluid dynamics of river dunes: a review and some future research directions. J. Geophys. Res. 110, F04S02 http://dx.doi.org/10.1029/2004JF000218.

Chen, Y., Wang, Z., Liu, Z., Zhu, D., 2012. 1D-2D coupled numerical model for shallow-water flows. J. Hydraul. Eng. 138 (2) http://dx.doi.org/10.1061/(ASCE)HY.1943-7900.0000481.

Cooper, J.R., Wainwright, J., Parsons, A.J., Onda, Y., Fukuwara, T., Obana, E., Kitchener, B., Long, E.J., Hargrave, G.H., 2012. A new approach for simulating the redistribution of soil particles by water erosion: a marker-in-cell model. J. Geophys. Res. – Earth Surf. 117, F04027 http://dx.doi.org/10.1029/2012JF002499.

CTI Engineering, 2007. Report on the Investigation for Planning of the Management of the lower Abukuma River, Japan. CTI Engineering Co., Ltd. in Japanese.

CTI Engineering, 2011. Report on the Consideration of Hazard Water Level in Abukuma and Natori River, Japan in 2011. CTI Engineering Co., Ltd in Japanese.

CTI Engineering, 2012. Report on the Consideration of Planning the Lower Abukuma River in 2012. CTI Engineering Co., Ltd in Japanese.

Ferguson, R.I., Parsons, D.R., Lane, S.N., hardy, R.J., 2003. Flow in meander bends with recirculation at the inner bank. Water Resour. Res. 39 (11), 1322, http://dx.doi.org/10.1029/2003WR001965.

Garcia, M.H., 2008. Sedimentation Engineering: Processes, Measurements, Modeling, and Practice. ASCE Publications, 1132pp.

Glysson, G.D., 1987. Sediment-transport Curves. U.S. Geological Survey, pp. 87–218. Open-File Report.

He, Q., Walling, D.E., 1996. Interpreting particle size effects in the adsorption of ^{137}Cs and unsupported ^{210}Pb by mineral soils and sediments. J. Environ. Radioact. 30 (2), 117–137.

Hean, C.J., 2008. The Dynamics of Coastal Models. Cambridge University Press. ISBN 978-0-521-80740-1.

International Atomic Energy Agency, 2006. Radiological Conditions in the Dnieper River Basin. In: Radiological Assessment Reports Series, 185pp.

Itakura, T., Kishi, T., 1980. Open channel flow with suspended sediments. J. Hydraulic Div. 106 (8), 1325–1343.

Iwagaki, Y., 1956. Hydrodynamical study on critical tractive force. Trans. Jpn. Soc. Civ. Eng. 41, 1–21, in Japanese.

Jang, C.L., Shimizu, Y., 2005. Numerical simulation of relatively wide shallow channels with erodible banks. J. Hydraulic Eng. 131, 565–575.

Japan Atomic Energy Agency, 2013a. Study on a Method for Understanding the Long-term Influence of Radioactive Substances Released in the Accident of Fukushima Dai-ichi Nuclear Power Plant Disaster: Progress Report, vol. 3 in Japanese.

Japan Atomic Energy Agency, 2013b. The Research and Study Concerning the Secondary Distribution Status of the Radioactive Substances from the Fukushima Dai-ichi Nuclear Power Plant Disaster, vol. 2. Progress report.

Kato, H., Onda, Y., Teramage, M., 2012. Depth distribution of ^{137}Cs, ^{134}Cs, and ^{131}I in soil profile after Fukushima Dai-ichi Nuclear Power Plant accident. J. Environ. Radioact. 111, 59–64.

Kimura, I., Uijttewaal, W., Hosoda, T., Ali, M., 2009. URANS computations of shallow grid turbulence. J. Hydraulic Eng. 135 (2), 118–131.

Kimura, I., Onda, S., Hosoda, T., Shimizu, Y., 2010. Computations of suspended sediment transport in a shallow side-cavity using depth-averaged 2D models with effects of secondary currents. J. Hydro-Environ. Res. 4 (2), 153–161.

Ministry of education, culture, sports, science and technology (MEXT), 2011. The 4th Airborne Survey Result of air Dose Level by MEXT. http://radioactivity.nsr.go.jp/ja/contents/5000/4901/24/1910_1216.pdf (in Japanese).

Nabi, M., de Vriend, H.J., Mosselman, E., Sloff, C.J., Shimizu, Y., 2012. Detailed simulation of morphodynamics: 1. Hydrodynamic model. Water Resour. Res. 48, W12523 http://dx.doi.org/10.1029/2012WR011911.

Nabi, M., de Vriend, H.J., Mosselman, E., Sloff, C.J., Shimizu, Y., 2013a. Detailed simulation of morphodynamics: 2. Sediment pickup, transport, and deposition. Water Resour. Res. 49 http://dx.doi.org/10.1002/wrcr.20303.

Nabi, M., de Vriend, H.J., Mosselman, E., Sloff, C.J., Shimizu, Y., 2013b. Detailed simulation of morphodynamics: 3. Ripples and dunes. Water Resour. Res. http://dx.doi.org/10.1002/wrcr.20457.

Nino, Y., Garcia, M., 1996. Experiments on particle-turbulence interactions in the near wall region of an open channel flow: implications for sediment transport. J. Fluid Mech. 326, 285–319.

Nippon Koei, 2012. Report on Investigations of Sediment Transport in Abukuma River basin, Japan in 2012. Nippon Koei Co., Ltd. in Japanese.

Onishi, Y., 1981. Sediment-contaminant transport model. J. Hydraulic Div. ASCE 107 (9), 1089–1107.

Rouse, H., 1937. Modern conceptions of the mechanics of fluid turbulence. Trans. ASCE 102, 463–543.

Rubey, W.W., 1933. Settling velocity of gravel, sand and silt particles. Am. Jour. Sci. 25, 325–338.

Saint-Venant, A., 1871. Théorie du mouvement non permanent des eaux, avec application aux crues des rivières et à l'introduction des marées dans leur lit. Comptes Rendus Séances l'Académie Sci. Paris 73, 147–154, 237–240.

Sanada, Y. and Torii, T. Aerial Radiation Monitoring around Fukushima Dai-ichi Nuclear Power Plant using an Unmanned Helicopter. (submitted in this issue).

Smith, H.G., Dragovich, D., 2009. Interpreting sediment delivery processes using suspended sediment-discharge hysteresis patterns from nested upland catchments, south-eastern Australia. Hydrol. Process. 23 (17), 2415–2426.

Tanaka, K., Iwatani, H., Sakaguchi, A., Fan, Q. and Takahashi, Y. Size-dependent Distribution of Radiocesium in Riverbed Sediments and its Relevance to the Migration of Radiocesium in River Systems after the Fukushima Daiichi Nuclear Power Plant accident. (submitted to this issue)

Venditti, J.G., Bennett, S.J., 2000. Spectral analysis of turbulent flow and suspended sediment transport over dunes. J. Geophys. Res. 105 (C9), 22035–22047 http://dx.doi.org/10.1029/2000JC900094.

Water Information System, 2013. Ministry of Land, Infrastructure and Transport, Japan. http://www1.river.go.jp/. in Japanese.

Wongsa, S., Shimizu, Y., 2004. Modelling artificial channel and land-use changes and their impact on floods and sediment yield to the Ishikari basin. Hydrol. Process. 18, 1837–1852.

Wu, W., 2007. Computational River Dynamics. CRC Press, 494pp.

Zheleznyak, M.J., Demchenko, R.I., Khursin, S.L., Kuzmenko, Y.I., Tkalich, P.V., Vitiuk, N.Y., 1992. Mathematical modeling of radionuclide dispersion in the Pripyat–Dnieper aquatic system after the Chernobyl accident. Sci. Total Environ. 112 (1), 89–112.

Please cite this article in press as: Iwasaki, T., et al., Computational modeling of ^{137}Cs contaminant transfer associated with sediment transport in Abukuma River, Journal of Environmental Radioactivity (2014), http://dx.doi.org/10.1016/j.jenvrad.2014.05.012